



# Effect of Non-Linear Radiation on Unsteady Convective Heat and Mass Transfer Flow past a Stretching surface with Hall Effects, Thermo-Diffusion, Radiation Absorption in the presence of Non-Uniform Heat Source with Constant Heat and Mass Flux

K.Kalpana<sup>1</sup> and Dr.M.Sreevani<sup>2</sup>

<sup>1</sup>Research scholar in Mathematics, Rayalaseema University, Kurnool, A.P

<sup>2</sup>Assistant Professor, Mathematics, S.K.University, Anantapur, A.P

**Abstract :** We study the effect of non-linear thermal radiation on unsteady convective heat and mass transfer flow of a viscous electrically conducting fluid past a stretching sheet in the presence of non-uniform heat source. The equations governing the flow of heat and mass transfer have been solved by Galerkin finite element analysis with three noded line segments.

**Keywords :** Radiation, Heat and Mass transfer, stretching sheet, thermo-diffusion, Heat source.

## 1. INTRODUCTION

Mixed convection boundary layer flow of a binary mixture of fluids with heat and mass transfer past a continuous moving surface has attracted considerable attention in the past several decades, due to its many important engineering and industrial applications (14,21)

In combined heat and mass transfer processes, the thermal energy flux resulting from concentration gradients is referred to as the Dufour or diffusion thermal effect. Similarly, the Soret or thermo-diffusion effect is the contribution to the mass fluxes due to temperature gradients. Moreover, when chemical species are introduced at a surface in the fluid domain with different (lower) density than the surrounding fluid, both Soret (thermo-diffusion) and Dufour (diffusion-thermal) effects can be influential. The effect of diffusion-thermal and thermal diffusion of heat and mass has been developed from the kinetic theory of gases by Champa and Cowling (6) and Hirshfelder et al. (13) They explained the phenomena and derived the necessary formulas to calculate the thermal diffusion coefficient and the thermal-diffusion factor for monatomic gases or for polyatomic gas mixtures. Several researchers (Kafousias and Williams (17) , Alam and Rahman (1) , Anghel et al. (3), Postelnicu (18), Alam et al. (2) , Beg et al. (5) )have studied the thermal diffusion and the diffusion-thermal effects on mixed free-forced convective and mass transfer steady laminar boundary layer flow, over a vertical flat plate under different conditions.

In all these investigations the electrical conductivity of the fluid was assumed to be uniform. However, in an ionized fluid where the density is low and/or magnetic field is very strong, the conductivity normal to the magnetic field is reduced due to the spiraling of electrons and ions about the magnetic lines of force before collisions take place and a current induced in a direction normal to both the electric and magnetic fields. This phenomenon available in the literature is known as Hall Effect. Thus the study of MHD viscous flows, heat and mass transfer with Hall currents has important bearing in the engineering applications. Hall effect on MHD boundary layer flow over a continues semi-infinite flat plate moving with a uniform velocity in its own plane in an incompressible viscous and electrically conducting fluid in the presence of a uniform transverse magnetic field were investigated by Watanabe and Pop [26]. The effect of Hall current on the study MHD flow of an electrically conducting, incompressible Burger's fluid between two parallel electrically insulating infinite plane was studied by Rana et. al. [19].

In all the above studies the physical situation is related to the process of uniform stretching sheet. For the development of more physically realistic characterization of the flow configuration it is very useful to introduce unsteadiness into the flow, heat and mass transfer problems. The working fluid heat generation or absorption effects are very crucial in monitoring the heat transfer in the regions, heat removal from nuclear fuel debris, underground disposal of radioactive waste material, storage of food stuffs, exothermic chemical reactions and dissociating fluids in packed-bed reactors. This heat source can occurs in the form of a coil or battery. Very few studies have been found in literature on unsteady boundary flows over a stretching sheet by taking heat generation/absorption into the account. Wang [25] was first studied the unsteady boundary layer flow of a liquid film over a stretching sheet. Elbashbeshy and Bazed [11] have presented the heat transfer over an unsteady stretching surface. Tsai et.al [24] has discussed flow and heat transfer characteristics over an unsteady stretching surface by taking heat source into the account. Ishak et al [15] analyzed the effect of prescribed wall temperature on heat transfer flow over an unsteady stretching permeable surface. Ishak [16] has presented unsteady

MHD flow and heat transfer behavior over a stretching plate. Recently, Dulal pal [8] has described the analysis of flow and heat transfer over an unsteady stretching surface with non-uniform heat source/sink and thermal radiation. Dulal pal et al. [9] have presented MHD non-Darcian mixed convection heat and mass transfer over a non-linear stretching sheet with Soret–Dufour effects, heat source/sink and chemical reaction. Salem and Aziz[20] analysed the effect of Hall current and chemical reaction on the steady flow, heat and mass transfer laminar of a viscous, electrically conducting fluid over a continuously stretching surface in the presence of heat generation/absorption. Aziz[4] investigated the flow and heat transfer of a viscous fluid flow over an unsteady stretching surface with Hall effects. Recently Sarojamma et al(22,23) have discussed the effect of Hall current on the flow induced by a stretching surface.

In this paper, we study the effect of non-linear thermal radiation on unsteady convective heat and mass transfer flow of a viscous electrically conducting fluid past a stretching sheet in the presence of non-uniform heat source. The equations governing the flow of heat and mass transfer have been solved by Galerkin finite element analysis with three noded line segments. The velocity, temperature and concentration have been analysed for different values of  $m, A1, B1, Sr, Nr, Sr, Q_1$  and  $A$ . The rate of heat and mass transfer on the plate has been evaluated numerically for different variations.

**2. FORMULATION OF THE PROBLEM:**

We analyse the unsteady convective heat and mass transfer flow of an electrically conducting fluid past a stretching sheet with the plane at  $y=0$  and the flow is confined to the region  $y>0$ . A schematic representation of the physical model is exhibited in fig.1. We choose the frame of reference  $O(x,y,z)$  such that the  $x$ -axis is along the direction of motion of the surface, the  $y$ -axis is normal to the surface and  $z$ -axis transverse to the  $(x-y)$  plane. An uniform magnetic field of strength  $H_0$  is applied in the positive  $y$ -direction. The surface of the sheet is assumed to have a variable temperature  $T_w(x)$ , while the ambient fluid has a uniform temperature  $T_\infty$ , where  $T_w(x) > T_\infty$  corresponds to a heated plate and  $T_w(x) < T_\infty$ , corresponds to a cooling plate. The effects of thermo-diffusion, thermal radiation, Hall currents, viscous dissipation, radiation absorption and the first order chemical reaction are considered. We consider Hall effects into consideration and assume the electron pressure gradient, the ion-slip and the thermo-electric effects are negligible. Using boundary layer approximation, Boussinesq’s approximation, Rosseland approximation the basic equations governing the flow, heat and mass transfer are

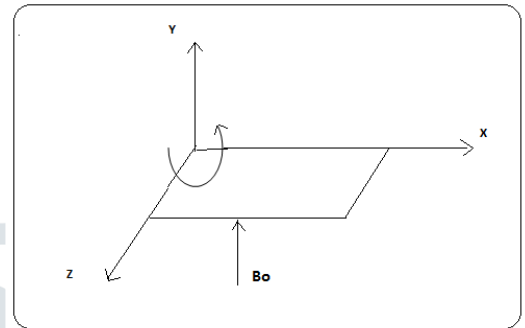


Fig.1 : Physical Configuration of the Problem

The equation of Continuity is

$$\frac{\partial u}{\partial x} + \frac{\partial v}{\partial y} = 0 \tag{2.1}$$

The Momentum equations are

$$\frac{\partial u}{\partial t} + u \frac{\partial u}{\partial x} + v \frac{\partial u}{\partial z} = \nu \frac{\partial^2 u}{\partial y^2} + \beta g(T - T_\infty) + \beta^* g(C - C_\infty) - \left(\frac{\mu}{k}\right)u - \frac{\sigma B_0^2}{\rho(1+m^2)}(u + mw) \tag{2.2}$$

$$\frac{\partial w}{\partial t} + u \frac{\partial w}{\partial x} + v \frac{\partial w}{\partial z} = \nu \frac{\partial^2 w}{\partial y^2} - \left(\frac{\mu}{k}\right)v + \frac{\sigma B_0^2}{\rho(1+m^2)}(mu - w) \tag{2.3}$$

The energy equation is

$$\rho C_p \left( \frac{\partial T}{\partial t} + u \frac{\partial T}{\partial x} + v \frac{\partial T}{\partial y} \right) = k_f \frac{\partial^2 T}{\partial y^2} + q''' - \frac{\partial(q_R)}{\partial y} + \mu \left( \left( \frac{\partial u}{\partial y} \right)^2 + \left( \frac{\partial w}{\partial y} \right)^2 \right) + \sigma B_0^2 (u^2 + w^2) + Q_1'(C - C_\infty) \tag{2.4}$$

The diffusion equation is

$$\left( \frac{\partial C}{\partial t} + u \frac{\partial C}{\partial x} + v \frac{\partial C}{\partial y} \right) = D_B \frac{\partial^2 C}{\partial y^2} - k_0(C - C_\infty) + \frac{D_m K_T}{T_m} \frac{\partial^2 T}{\partial y^2} \tag{2.5}$$

The coefficient  $q'''$  is the rate of internal heat generation (>0) or absorption(<0). The internal heat generation /absorption  $q'''$  is modeled as

$$q''' = \left( \frac{ku_s}{xv} \right) [A1(T_w - T_\infty) f'(\eta) + B1(T - T_\infty)] \tag{2.6}$$

Where  $A1$  and  $B1$  are coefficients of space dependent and temperature dependent internal heat generation or absorption respectively. It is noted that the case  $A1 > 0$  and  $B1 > 0$ , corresponds to internal heat generation and that  $A1 < 0$  and  $B1 < 0$ , the case corresponds to internal heat absorption case.

The radiation heat term by using the Rosseland approximation is given by

$$q_r = -\frac{4\sigma^* \partial T'^4}{3\beta_R \partial y} \quad (2.7)$$

$$T'^4 \cong 4TT_\infty^3 - 3T_\infty^4 \quad (2.8)$$

$$\frac{\partial q_R}{\partial z} = -\frac{16\sigma^* T_\infty^3}{3\beta_R} \frac{\partial^2 T}{\partial y^2} \quad (2.9)$$

The non-dimensional temperature  $\theta(\eta) = \frac{T - T_\infty}{T_w - T_\infty}$  can be simplified as

$$T = T_\infty(1 + (\theta_w - 1)\theta) \quad (2.10)$$

Where  $\theta = \frac{T_w - T}{T_w - T_\infty}$  is the temperature parameter. Using (2.6) & (2.10), equation (2.4) reduces to

$$\rho C_p \left( \frac{\partial T}{\partial t} + u \frac{\partial T}{\partial x} + v \frac{\partial T}{\partial y} \right) = k_f \frac{\partial^2 T}{\partial y^2} + q'' - \frac{\partial(q_R)}{\partial y} + \mu \left( \left( \frac{\partial u}{\partial y} \right)^2 + \left( \frac{\partial w}{\partial y} \right)^2 \right) + \sigma B_o^2 (u^2 + w^2) + Q_1 (C - C_\infty) \quad (2.11)$$

where T is the temperature and C is the concentration in the fluid.  $k_f$  is the thermal conductivity,  $C_p$  is the specific heat at constant pressure,  $\beta$  is the coefficient of thermal expansion,  $\beta^*$  is the volumetric expansion with concentration,  $Q_1^1$  is the radiation absorption coefficient,  $q_r$  is the radiative heat flux,  $k_c$  is the chemical reaction coefficient,  $D_B$  is the molecular viscosity,  $D_m$ ,  $K_T$ ,  $T_m$ ,  $k$  is the porous permeability parameter.

The boundary conditions for this problem can be written as

$$u = U(x, t), v = V_w(x, t), w = 0, \frac{\partial T}{\partial y} = -\frac{q_w}{k_f}, \frac{\partial C}{\partial y} = -\frac{m_w}{D_m} \quad \text{on } y = 0 \quad (2.12)$$

$$u = w = 0, T = T_\infty, C = C_\infty \quad \text{as } y \rightarrow \infty \quad (2.13)$$

Where u and v are the fluid velocity components along x and y-axis respectively and t is the time.  $v_w(x, t) = -\left(\frac{\nu U_w}{x}\right)^{1/2} f(0)$  represents the mass transfer at the surface with  $V_w > 0$  for injection and  $V_w < 0$  for suction. The flow is caused by the stretching of the sheet which moves in its own plane with the surface velocity  $U_w(x, t) = \frac{ax}{(1-ct)}$ , where a (stretching rate) and c are the positive

constants having dimension  $\text{time}^{-1}$  (with  $t < 1, c \geq 0$ ). It is noted that the stretching rate  $\frac{a}{(1-ct)}$  increases with time, since  $a > 0$ . The surface temperature and concentration of the sheet varies with the distance x from the slot and time t in the form so that surface temperature

$$T_w(x, t) = T_\infty + \frac{ax^2}{2\nu(1-ct)^{3/2}} \quad \text{and} \quad \text{surface concentration } C_w(x, t) = C_\infty + \frac{ax^2}{2\nu(1-ct)^{3/2}} \quad \text{where } a \geq 0. \quad \text{The particular form of}$$

$U_w(x, t), T_w(x, t)$  and  $C_w(x, t)$  has been chosen in order to derive a similarity transformation which transforms the governing partial differential equations (2)-(5) into a set of highly nonlinear ordinary differential equations.

The radiation heat term (Brewster) by using the Rosseland approximation is given by

$$q_r = -\frac{4\sigma^* \partial T'^4}{3\beta_R \partial y} \quad (2.14)$$

$$T'^4 \cong 4TT_\infty^3 - 3T_\infty^4 \quad (2.15)$$

$$\frac{\partial q_R}{\partial z} = -\frac{16\sigma^* T_\infty^3}{3\beta_R} \frac{\partial^2 T}{\partial y^2} \quad (2.16)$$

The non-dimensional temperature  $\theta(\eta) = \frac{T - T_\infty}{T_w - T_\infty}$  can be simplified as  $T = T_\infty(1 + (\theta_w - 1)\theta)$

Where  $\theta = \frac{T_w - T}{T_w - T_\infty}$  is the temperature parameter. The stream function  $\psi(x, t)$  is defined as:

$$u = \frac{\partial \psi}{\partial y} = \frac{ax}{(1-ct)} f'(\eta), v = -\frac{\partial \psi}{\partial x} = \frac{av}{(1-ct)} f(\eta) \quad (2.17)$$

we introduce the similarity variables (Dulal Pal [8]) as

$$\eta = \sqrt{\frac{a}{(1-ct)}} y \quad (2.18)$$

$$\psi(x, y, t) = \left(\frac{va}{1-ct}\right)^{1/2} x f(\eta), w = \left(\frac{ax}{1-ct}\right) g(\eta) \quad (2.19)$$

$$T(x, t, t) = T_\infty + \frac{ax^2}{2\nu(1-ct)^{3/2}} \theta(\eta), \theta(\eta) = \frac{T - T_\infty}{T_w - T_\infty} \quad (2.20)$$

$$C(x, t, t) = C_\infty + \frac{ax^2}{2\nu(1-ct)^{3/2}} \phi(\eta), \phi(\eta) = \frac{C - C_\infty}{C_w - C_\infty} \quad (2.21)$$

$$B^2 = B_0^2(1-ct)^{-1} \quad (2.22)$$

Using equations (2.18)- (2.22) into equations(2.2),(2.3),(2.5)and (2.7) we get

$$f''' + f f'' - f'^2 - S(f' + 1.5f'') + G(\theta + N\phi) - D^{-1}f' - \frac{M^2}{1+m^2}(f' + mg) = 0 \quad (2.23)$$

$$g'' + fg' - f'g - S(g' + 1.5g'') - D^{-1}g + \frac{M^2}{1+m^2}(mf' - g) = 0 \quad (2.24)$$

$$Rd(1 + (\theta_w - 1)\theta^3)\theta'' + Pr(f\theta' - 2f'\theta - 0.5S(3\theta + \eta\theta')) + Pr(A_1f' + B_1\theta) + Ec((f'')^2 + (g')^2) + \frac{M^2}{1+m^2}((f')^2 + g^2) + Q_1\phi = 0 \quad (2.25)$$

$$\phi'' + Sc(f\phi' - 2f'\phi - 0.5S(3\phi + \eta\phi')) - Sc\gamma\phi + ScSo\theta'' = 0 \quad (2.26)$$

where  $S=c/a$  is the unsteadiness parameter.  $M = \frac{\sigma B_0^2}{\rho a}$  is the magnetic parameter,

$D^{-1} = \frac{\nu}{ak}$  is the inverse Darcy parameter,  $G = \frac{\beta g(T_w - T_\infty)}{U_w \nu_w^2}$  is the thermal buoyancy parameter,  $N = \frac{\beta^*(C_w - C_\infty)}{\beta(T_w - T_\infty)}$  is the

buoyancy ratio,  $Pr = \frac{\mu C_p}{k_f}$  is the Prandtl number,  $Ec = \frac{U_w^2}{C_p(T_w - T_\infty)}$  is the Eckert number,  $Q_1 = \frac{\nu Q_1'}{\nu_w^2}$  is the Radiation

absorption parameter,  $Sc = \frac{\nu}{D_B}$  is the Schmidt number,  $m = \omega_e \tau_e$  is the Hall parameter,  $\gamma = \frac{k_0 \nu}{\nu_w^2}$  is the chemical reaction

parameter and  $So = \frac{D_m K_T (T_w - T_\infty)}{\nu T_m (C_w - C_\infty)}$  is the Soret parameter,  $Rd = \frac{4\sigma T_\infty^3}{\beta_R k_f}$  is the radiation parameter.

It is pertinent to mention that  $\gamma > 0$  corresponds to a degenerating chemical reaction while  $\gamma < 0$  indicates a generation chemical reaction.

The transformed boundary conditions (2.8)&(2.9) reduce to

$$f'(0) = 1, f(0) = fw, g(0) = 0, \theta'(0) = -1, \phi'(0) = -1 \quad (2.27)$$

$$f'(\infty) \rightarrow 0, g(\infty) \rightarrow 0, \theta(\infty) \rightarrow 0, \phi(\infty) \rightarrow 0 \quad (2.28)$$

where  $fw = \frac{\nu_w}{\sqrt{av}}$  is the mass transfer coefficient such that  $fw > 0$  represents suction and  $fw < 0$  represents injection at the surface..

### 3.SKIN FRICTION,NUSELT NUMBER and SHERWOOD NUMBER

The physical quantities of engineering interest in this problem are the skin friction coefficient  $C_f$ , the Local Nusselt number  $Nu_x$ , the Local Sherwood number  $Sh_x$  which are expressed as

$$\frac{1}{2} C_f \sqrt{R_{ex}} = f''(0), \frac{1}{2} C_{fz} \sqrt{R_{ez}} = g'(0),$$

$$Nux / \sqrt{R_{ex}} = 1 / \theta(0), Shx / \sqrt{R_{ex}} = 1 / \phi(0)$$

Where  $\mu = \frac{k}{\rho C_p}$  is the dynamic viscosity of the fluid and  $Re_x$  is the Reynolds number.

For the computational purpose and without loss of generality  $\infty$  has been fixed as  $\eta_{\max}=8$ . The whole domain is divided into 11 line elements of equal width, each element being three noded.

#### 4. METHOD OF SOLUTION

The equations (2.23-2.26) governing the flow, heat and mass transfer have been solved by using Galerkin finite element technique with quadratic interpolation functions. The local stiffness matrices are assembled by using inter element continuity, equilibrium conditions and boundary conditions. The ultimate coupled global matrices are solved to determine the unknown global values of velocity, temperature and concentration in the fluid region. In solving these matrices an iteration procedure has been adopted.

**COMPARISON:** Comparison of  $Nu(0)$  for  $M=m=G=N=Ec=Q1=Sc=fw=\gamma=0, A1=B1=0, So=0, \theta_w=0$

Pr	Chen(7)	Grubka and Bobba (12)	Aziz(4)	Sarojamma et al(23)	Present results
0.01	0.02942	0.0294	0.02948	0.02949	0.02947
0.72	1.08853	1.0885	1.08855	1.08857	1.08856
1.0	1.33334	1.3333	1.33333	1.33335	1.333339
3.0	2.50972	2.5097	2.50972	2.50974	2.509746
7.0	3.97150		3.97151	3.97152	3.971522
10.0	4.79686	4.7969	4.79687	4.79688	4.796879
100.0	15.7118	15.712	15.7120	15.7122	15.71229

#### 5. DISCUSSION OF THE NUMERICAL RESULTS

In order to validate the accuracy of the numerical scheme employed we have compared the local temperature gradient of the present analysis with those of Chen(7), Grubka and Bobba(12), Aziz(4) and Sarojamma et al(23) for different values of Prandtl number in absence of magnetic field, thermal and solutal buoyancy, radiation absorption, viscous dissipation and suction for steady flow  $M=Gr=N=\gamma=Q1=Ec=Sc=fw=A1=B1=0, So=\theta_w=0$  and presented in table.1 and are found to be in good agreement.

Figs.2a-2d represents the velocity, temperature and concentration with Hall parameter ( $m$ ). As mentioned above the Lorentz force has a retarding effect on the primary velocity, this retardation is enhanced with increase in the Hall parameter and hence the primary velocity is enhanced and consequently the momentum boundary layers become thicker. The secondary velocity increases as the Hall parameter increases. The effect of Hall parameter on temperature and concentration shows that the temperature reduces and the concentration enhances with increase in Hall parameter ( $m$ ). This is due to the reduction of thermal boundary layer and increasing the solutal boundary layer.

Figs.3a-3d represent the impact of thermal radiation on the velocities, temperature and concentration. It can be seen from the profiles that higher the radiative heat flux, larger the velocities, temperature and smaller the concentration. This is due to the fact that the thickness of the momentum and thermal boundary layers increases while the solutal boundary layer decreases with increase in the radiation parameter ( $Nr$ ).

Figs.4a-4d and 10a-10d represent the velocity, temperature and mass concentration with space dependent heat source and temperature dependent source. An increase in the space dependent source ( $A1>0$ ) enhances the velocities and temperature while the concentration reduces owing to the generation of energy in the boundary layer while in the case of heat absorption source ( $A1<0$ ), the primary, secondary velocities and the temperature reduce while the concentration enhances in the boundary layer in the boundary layer. In the case of temperature dependent generating source ( $B1>0$ ), the velocities, temperature enhance while the concentration reduces in the boundary layer and a reversed effect is noticed with  $B1<0$ .

Figs.5a-5d represent the variation of velocity, temperature and concentration with Soret parameter ( $Sr$ ). It is found that higher the thermo-diffusion effects larger the velocity, temperature and concentration in the entire boundary layer. This is due to the fact that an increase in  $Sr$  increases the thickness of the momentum, thermal and solutal boundary layers.

Figs.6a-6d represent the effect of radiation absorption ( $Q1$ ) on velocity, temperature and concentration. It is found that the primary and secondary velocity components increase with increase in  $Q1$ . An increase in  $Q1$  increases the thickness of the thermal and solutal boundary layers.

Figs.7a-7d illustrate the variation of velocities, temperature and concentration with temperature parameter ( $A$ ). Higher the values of temperature parameter smaller the velocities, temperature and larger the concentration in the boundary layer. Thus the non-linearity of thermal radiation leads to a reduction in velocity and temperature and increment in concentration.

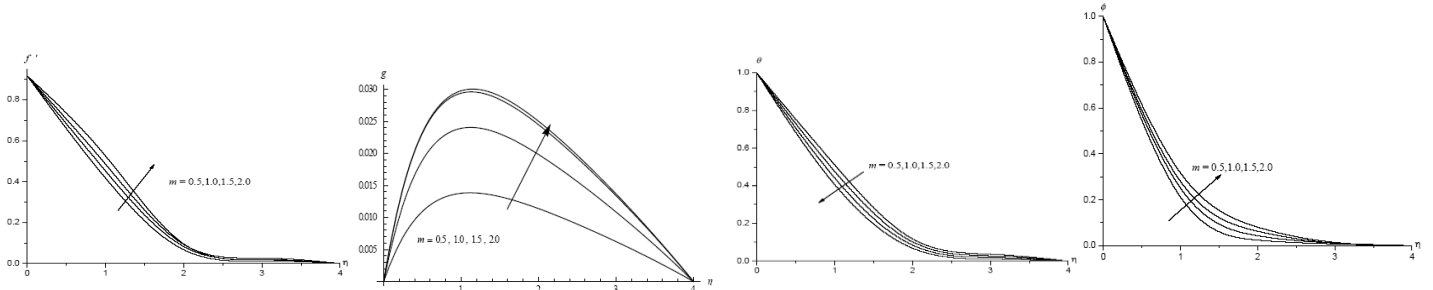


Fig. 2a Effect of  $m$  on  $f'(\eta)$   
 $Q1=0.5, A1=0.1, B1=0.1, Nr=0.5, Sr=0.5, A=1.05$

Fig. 2b Effect of  $m$  on  $g(\eta)$   
 $Nr=0.5, Q1=0.5, A1=0.1, B1=0.1, Sr=0.5, A=1.05$

Fig. 2c Effect of  $m$  on  $\theta(\eta)$   
 $Q1=0.5, A1=0.1, B1=0.1, Nr=0.5, Sr=0.5, A=1.05$

Fig. 2d Effect of  $m$  on  $\phi(\eta)$   
 $Q1=0.5, A1=0.1, B1=0.1, Nr=0.5, Sr=0.5, A=1.05$

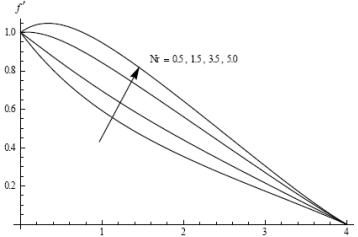


Fig. 3a Effect of  $Nr$  on  $f'(\eta)$   
 $m=0.5, Q1=0.5, A1=0.1, B1=0.1, Sr=0.5, A=1.05$

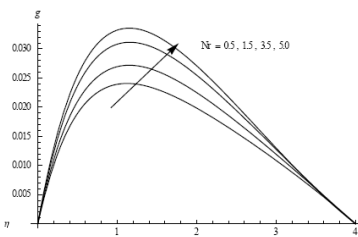


Fig. 3b Effect of  $Nr$  on  $g(\eta)$   
 $m=0.5, Q1=0.5, A1=0.1, B1=0.1, Sr=0.5, A=1.05$

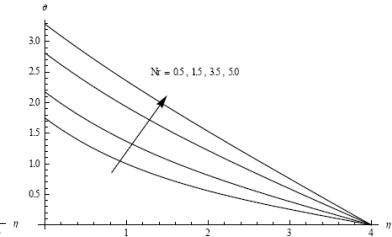


Fig. 3c Effect of  $Nr$  on  $\theta(\eta)$   
 $m=0.5, Q1=0.5, A1=0.1, B1=0.1, Sr=0.5, A=1.05$

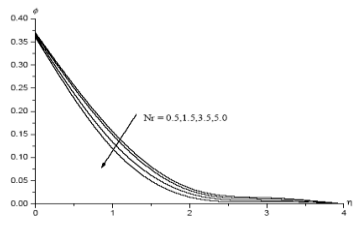


Fig. 3d Effect of  $Nr$  on  $\phi(\eta)$   
 $m=0.5, Q1=0.5, A1=0.1, B1=0.1, Sr=0.5, A=1.05$

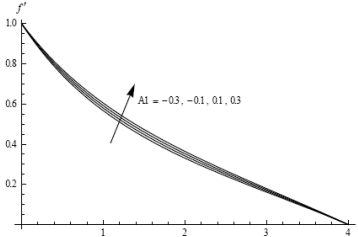


Fig. 4a Effect of  $A1$  on  $f'(\eta)$   
 $m=0.5, Q1=0.5, B1=0.1, Nr=0.5, Sr=0.5, A=1.05$

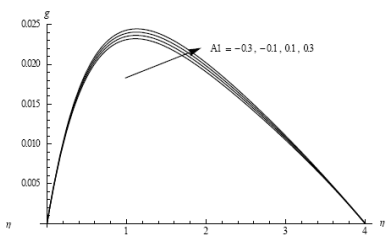


Fig. 4b Effect of  $A1$  on  $g(\eta)$   
 $m=0.5, Q1=0.5, B1=0.1, Nr=0.5, Sr=0.5, A=1.05$

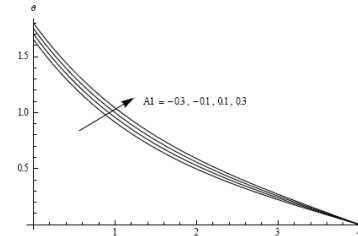


Fig. 4c Effect of  $A1$  on  $\theta(\eta)$   
 $m=0.5, Q1=0.5, B1=0.1, Nr=0.5, Sr=0.5, A=1.05$

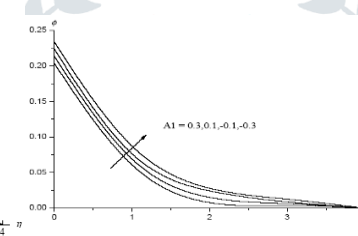


Fig. 4d Effect of  $A1$  on  $\phi(\eta)$   
 $m=0.5, Q1=0.5, B1=0.1, Nr=0.5, Sr=0.5, A=1.05$

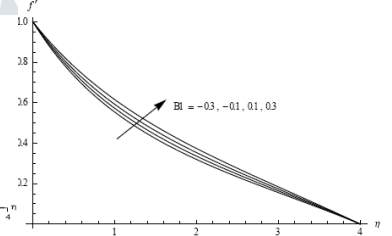


Fig. 5a Effect of  $B1$  on  $f'(\eta)$   
 $m=0.5, Q1=0.5, A1=0.1, Nr=0.5, Sr=0.5, A=1.05$

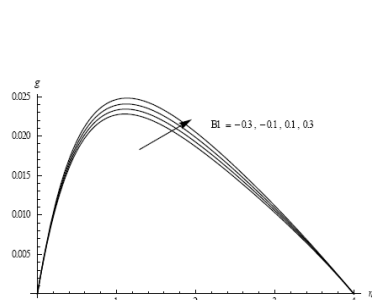


Fig. 5b Effect of  $B1$  on  $g(\eta)$   
 $m=0.5, Q1=0.5, A1=0.1, Nr=0.5, Sr=0.5, A=1.05$

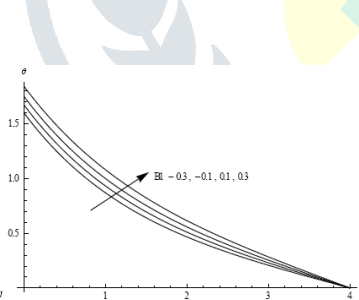


Fig. 5c Effect of  $B1$  on  $\theta(\eta)$   
 $m=0.5, Q1=0.5, A1=0.1, Nr=0.5, Sr=0.5, A=1.05$

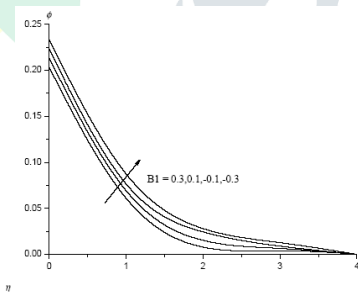


Fig. 5d Effect of  $B1$  on  $\phi(\eta)$   
 $m=0.5, \gamma=0.5, Q1=0.5, A1=0.1, Nr=0.5, Sr=0.5, A=1.05$

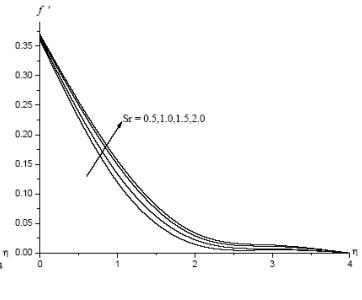


Fig. 6a Effect of  $Sr$  on  $f'(\eta)$   
 $m=0.5, Q1=0.5, A1=0.1, B1=0.1, Nr=0.5, A=1.05$

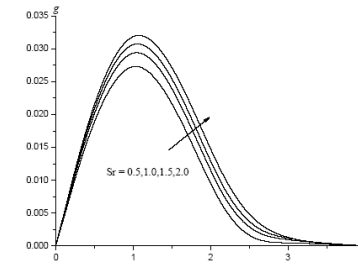


Fig. 6b Effect of  $Sr$  on  $g(\eta)$   
 $m=0.5, Q1=0.5, A1=0.1, B1=0.1, Nr=0.5, A=1.05$

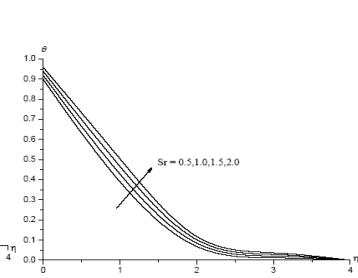


Fig. 6c Effect of  $Sr$  on  $\theta(\eta)$   
 $m=0.5, Q1=0.5, A1=0.1, B1=0.1, Nr=0.5, A=1.05$

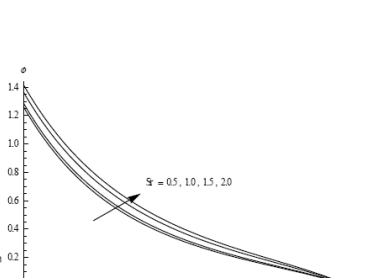


Fig. 6d Effect of  $Sr$  on  $\phi(\eta)$   
 $m=0.5, Q1=0.5, A1=0.1, B1=0.1, Nr=0.5, A=1.05$

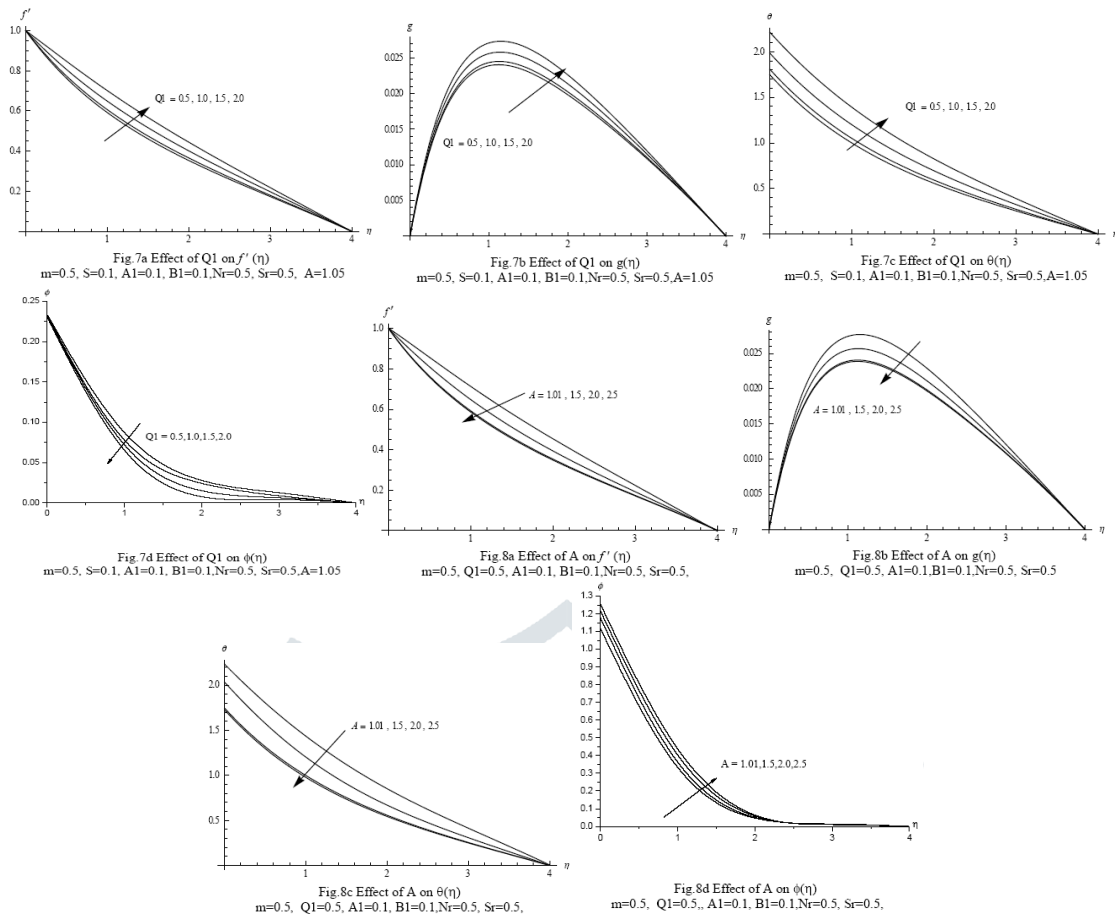


Table.2 : Stress components( $\tau_x, \tau_z$ ), Nusselt number( $Nu_0$ ), Sherwood number( $Sh$ ) on  $\eta=0$

Parameter	$\tau_x(0)$	$\tau_z(0)$	$Nu(0)$	$Sh(0)$	
m	0.5	-0.569761	0.0612648	0.571939	0.794719
	1.0	-0.544076	0.0771174	0.573295	0.794398
	1.5	-0.510811	0.0740387	0.575103	0.793972
	2.0	-0.2988049	0.0811392	0.580826	0.789703
Sr	0.5	-0.569761	0.0612648	0.571939	0.794719
	1.0	-0.566074	0.0613408	0.570798	0.778584
	1.5	-0.555098	0.0615665	0.567427	0.734103
	2.0	-0.109172	0.0752453	0.548854	0.718598
Q1	0.5	-0.569761	0.0612648	0.571939	0.794719
	1.0	-0.534153	0.0619732	0.552882	0.795299
	1.5	-0.430433	0.0639776	0.503534	0.797075
	2.0	-0.2581385	0.0640892	0.445337	0.803132
Nr	0.5	-0.569761	0.0612648	0.571939	0.794719
	1.5	-0.319023	0.0660878	0.459843	0.798582
	3.5	0.049152	0.0725579	0.355648	0.803653
	5.0	0.0398501	0.0800658	0.306583	0.804947
	0.03	-0.567241	0.0613133	0.570506	0.794777
A1	0.1	-0.569761	0.0612648	0.571939	0.794719
	0.3	-0.538577	0.0619039	0.555532	0.795085
	-0.1	-0.598835	0.0606634	0.588116	0.794368
	-0.3	-0.124927	0.0526481	0.581395	0.801802
B1	0.1	-0.569761	0.0612648	0.571939	0.794719
	0.3	-0.514461	0.0623827	0.543282	0.795442
	-0.1	-0.616644	0.0603015	0.598631	0.794092
	-0.3	-0.133836	0.0512272	0.60514	0.801513
A	1.01	-0.569761	0.0612648	0.571939	0.794719
	1.50	-0.582869	0.0609892	0.578564	0.794725
	2.00	-0.414431	0.0639611	0.491057	0.80024
	2.50	-0.278058	0.0669626	0.446958	0.804888
	7.00	-1.243451	0.0328148	1.15769	0.776565

The skin friction coefficients ( $\tau_x$ ) and ( $\tau_z$ ) are exhibited in table.2 for different values of  $m, A1, B1, Nr, Q1, Sr, A$ . An increase in the Hall parameter ( $m$ ) or Soret parameter ( $Sr$ ) reduces  $\tau_x$  and enhances  $\tau_y$  at the wall  $\eta=0$ . An increase in  $Q1$  reduces  $\tau_x$  and enhances  $\tau_y$  on the wall. An increase in space dependent/temperature dependent heat generating /absorbing source reduces  $\tau_x$  for  $A1(<0>0)$  or  $B1(<0>0)$ .  $\tau_y$  enhances at the wall with  $A1>0$  or  $B1>0$  while a reversed effect is noticed at the wall for  $A<0$  or  $B1<0$ . The variation of stress components with temperature parameter ( $A$ ) shows that an increase in  $A \leq 1.5$  enhances  $\tau_x$  and reduces  $\tau_y$  and for still higher  $A \geq 2.0$ , a reversed effect is noticed in their behaviour. Thus the non-linearity in thermal radiation leads to a reduction in the stress

component  $\tau_y$  and increment in  $\tau_x$  at the wall for smaller values of  $A$  and for higher values of  $A$   $\tau_x$  reduces and  $\tau_y$  enhances at the wall.

The rate of heat transfer (Nusselt number) at the wall  $\eta=0$  is exhibited in table.2. for different parametric variations. It is found that the rate of heat transfer increases Hall parameter( $m$ ). Higher the radiation absorption ( $Q_1$ ) or dissipative energy( $Ec$ ) or thermal radiation( $Nr$ ) smaller  $Nu$  on the wall.  $|Nu|$  increases with increase in the space dependent heat source/sink. Also it reduces with  $B_1 > 0$  and enhances with  $B_1 < 0$ . With respect to the Soret parameter  $So$ , we find that the rate of heat transfer reduces with increase in  $So$ . The rate of heat transfer at the wall enhances with increase in  $A \leq 1.5$  and reduces with higher values of  $A \geq 2.0$ . Thus non-linearity in thermal radiation leads to an enhancement in  $Nu$  for smaller values of  $A$  and reduces for higher values of  $A$ . The rate of mass transfer (Sherwood Number) at the wall  $\eta=0$  is shown in table.2 for different variations. An increase in Hall parameter( $m$ ) reduces the Sherwood number at the wall. The variation of  $Sh$  with radiation absorption parameter  $Q_1$  shows that  $|Sh|$  enhances with increase in  $Q_1$ . With reference to  $A_1$  and  $B_1$  we find that  $|Sh|$  enhances with increase in  $A_1$  or  $B_1$ . The rate of mass transfer increases with increase in  $Nr$  and reduces with Soret parameter  $Sr$ . The variation of  $Sh$  with temperature parameter( $A$ ) shows that higher the temperature parameter( $A \leq 1.5$ ) smaller  $Sh$  and for still higher  $A \geq 2.0$ , it enhances on the wall.

## CONCLUSIONS

The coupled equations governing the flow, heat and mass transfer have been solved by employing Finite element method. The velocity, temperature and concentrations are discussed graphically for different variations. The conclusions of this analysis are:

- 1) The velocity components, concentration enhances and the temperature reduces with increasing Grashof number  $G$ . The stress component  $\tau_x$ , Nusselt number and Sherwood number reduces while  $\tau_y$  increases with  $G$ .
- 2) Higher the Lorentz force smaller the primary velocity, larger the secondary velocity, temperature and smaller the concentration. The stress components, Nusselt number reduces and the rate of mass transfer enhances with  $M$ .
- 3) An increase in Hall parameter reduces the primary and secondary velocities, temperature reduces and concentration enhances. The stress component  $\tau_x$  enhances, Nusselt number, Sherwood number and the stress component  $\tau_y$  reduce at the wall.
- 4) An increase in the buoyancy ratio ( $N > 0$ ) enhances the velocities, temperature and concentration enhance while the stress components, Nusselt and Sherwood number reduces on the wall. The primary velocity, Nusselt and Sherwood number enhances while the secondary velocity, temperature, concentration and the stress components reduces with increase in  $N < 0$ .
- 5) The primary, secondary velocities, temperature enhance and concentration reduces with increase in  $A_1 > 0$  while they experience a reduction with  $A_1 < 0$ . An increase in  $B_1 > 0$  reduces the velocities, enhances the temperature and concentration. A reversed effect is noticed with  $B_1 < 0$ .
- 6) The velocity components, the temperature enhances, and concentration reduces with increase in  $Nr$ . The rate of heat transfer enhances while the Sherwood number reduces at the wall.
- 6) Lesser the molecular diffusivity smaller the velocities, temperature, concentration, and reduces  $\tau_y$  and reduces stress component  $\tau_x$ , Nusselt number and Sherwood number.
- 7) The velocity components, temperature and concentration reduces in degenerating chemical reaction case and enhance in the generating case. The stress component  $\tau_x$  and Sherwood number reduces in both the degenerating /generating cases, the Nusselt number reduces with  $\gamma > 0$  and enhances with  $\gamma < 0$ .
- 8) Higher the radiation absorption larger the velocities, temperature and smaller concentration. An increase in  $Q_1$  reduces  $\tau_x$ , enhances  $\tau_y$ ,  $Nu$  and  $Sh$ .
- 9) Increase in Soret parameter  $So$  increases the velocities, temperature and concentration,  $\tau_x$ , Sherwood number and reduces  $\tau_y$  and  $Nu$ .
- 10) Higher the dissipation smaller the velocities, and smaller temperature, concentration. The stress component  $\tau_y$  and rate of heat and mass transfer, reduces, the secondary velocity,  $\tau_x$  enhances on the wall.
- 10) An increase in Unsteady parameter  $s$  reduces the velocities, concentration and reduces the temperature and in the flow region. The stress component  $\tau_x$ , the rate of mass transfer enhances and the stress component  $\tau_y$  and Nusselt number reduces on the wall.
- 11) Higher the suction parameter ( $fw > 0$ ) smaller the velocities, temperature, and Sherwood number and larger the concentration, stress components and Nusselt number. An increase in  $fw < 0$ , increases primary velocity, reduces the secondary velocity, temperature, and concentration,  $\tau_x$ ,  $\tau_y$  and Sherwood number and decreases the Nusselt number.
- 12) An increase in  $Pr$  reduces the velocities, temperature and enhances the concentration.  $\tau_x$  and  $Nu$  enhances and  $\tau_y$ ,  $Nu$  reduces on the wall with  $Pr$ .

## REFERENCES

1. Alam, M. S., and Rahman, M. M: Dufour and Soret effects on mixed convection flow past a vertical porous flat plate with variable suction, *Nonlinear Anal. Model. Control*, 11, 3–12. (2006).
2. Alam, M. S., Rahman, M. M., Ferdows, M., Kaino, K., Mureithi, E., and Postelnicu, A: Diffusion-thermo and thermal-diffusion effects on free convective heat and mass transfer flow in a porous medium with time dependent temperature and concentration, *Int. J. Appl. Eng. Res.*, 2(1), 81–96. (2007).
3. Anghel, M., Takhar, H. S., and Pop, I: Dufour and Soret effects on free convection boundary-layer over a vertical surface embedded in a porous medium, *Stud. Univ. Babeş-Bolyai Math.*, 45(4), 11–21 (2000).
4. Aziz, M. A. E: Flow and heat transfer over a unsteady stretching surface with Hall effects., *Mechanica*, V.45, pp.97-109 (2010)
5. Beg, O. A., Bakier, A. Y., and Prasad, V. R.: Numerical study of free convection magnetohydrodynamic heat and mass transfer from a stretching surface to a saturated porous medium with Soret and Dufour effects, *Comput. Mater. Sci.*, 46, 57–65 (2009).
6. Chapman, S., and Cowling, T. G: (1952). *The Mathematical Theory of Non-uniform Gases*, 2nd ed., Cambridge Univ. Press, Cambridge (1952).
7. Chen C.H: Laminar mixed convection adjacent to vertical continuously stretching sheets, *Heat and Mass transfer*, V.33, pp.471-476 (1998)
8. Dulal Pal: Combined effects of non-uniform heat source/sink and thermal radiation on heat transfer over an unsteady stretching permeable surface, *Commun Nonlinear Sci Numer Simulat*, 16, 1890–1904, (2011.)



9. Dulal Pal, Hiranmoy Mondal: MHD non-Darcian mixed convection heat and mass transfer over a non-linear stretching sheet with Soret–Dufour effects and chemical reaction, *International Communications in Heat and Mass Transfer* 38, 463–467( 2011).
10. El-Aziz, M. A: Flow and heat transfer over an unsteady stretching surface with Hall effects, *Mechanica*, V.45, pp.97-109(2010)
11. Elbashaeshy EMA, and Bazid MAA, Heat transfer over an unsteady stretching surface, *Heat Mass Transfer*, 41, 1–4(2004).
12. Grubka, L.J and Bobba, K.M: Heat transfer characteristics of a continuous stretching surface with variable temperature, *ASME, J. Heat Transfer*, V.107, pp.248(1985)
13. Hirshfelder, J. O., Curtis, C. F., and Bird, R. B: *Molecular Theory of Gases and Liquids*, 1249, John Wiley, New York. (1954)
14. Jaluria, Y: *Natural Convection Heat and Mass Transfer*, 326, Pergamon Press, Oxford. (1980).
15. Ishak A, Nazar R, and Pop I, Heat transfer over an unsteady stretching permeable surface with prescribed wall temperature, *Nonlinear Anal: Real World Appl*, 10, 2909–13(2009).
16. Ishak A, Unsteady MHD flow and heat transfer over a stretching plate, *J. Applied Sci*, 10(18), 2127-2131(2010).
17. Kafoussias, N. G., and Williams, E. W: Thermal-diffusion and diffusion-thermo effects on mixed free-forced convective and mass transfer boundary layer flow with temperature dependent viscosity, *Int. J. Eng.*, 33, 1369–1384 (1995).
18. Postelnicu, A.: (2007). Influence of chemical reaction on heat and mass transfer by natural convection from vertical surfaces in porous media considering Soret and Dufour effects, *Heat Mass Transfer*, 43, 595–602(2007)
19. Rana, M.A, Siddiqui, A.M and Ahmed, N : Hall effect on Hartmann flow and heat transfer of a burger’s fluid. *Phys. Letters A* 372, pp. 562-568(2008).
20. Salem, A.M, Abd El-Aziz, M: Effect of Hall currents and chemical reaction on hydromagnetic flow of a stretching vertical surface with internal heat generation/absorption, *Applied Mathematical Modelling*, V.32, pp.1236-1254(2008)
21. Schlichting, H: (1979). *Boundary Layer Theory*, 6th ed., 817, McGraw-Hill, New York (1979)..
22. Sarojamma, G, Mahaboobjan, S and Sreelakshmi, K: Effect of Hall current on the flow induced by a stretching surface., *Int. Jour. Scientific and Innovative Mathematical research*, V.3(3), pp.1139-1148(2015)
23. Sarojamma, G, Syed Mahaboobjan and V. Nagendramma : Influence of hall currents on cross diffusive convection in a MHD boundary layer flow on stretching sheet in porous medium with heat generation. *IJMA*, 6(3), pp: 227-248 (2015).
24. Tsai R, Huang K. H, and Huang J. S, Flow and heat transfer over an unsteady stretching surface with non-uniform heat source, *Int. Commun. Heat Mass Transfer*, 35, 1340-1343(2008).
25. Wang CY: Liquid film on an unsteady stretching surface, *Q Appl Math*, 48, 601–10(1990).
26. Watanabe T and Pop I: Hall effects on magnetohydrodynamic boundary layer flow over a continuous moving flat plate. *Acta Mech*. 108, pp. 35-47, (1995)

